International Journal of Scientific Research and Management Studies (IJSRMS)
ISSN: 2349-3771 **Volume 2 Issue 4, pg: 164-174**

DESIGN OF PLASTIC & STEEL COMPONENT FOR REQUIRED LIFE BY EXPERIMENTAL AND FINITE ELEMENT METHOD

Sachin V. Shah
Department of Mechanical Engineering, Rajarshee Shahu College of Engineering, Pune University, Pune 411033, India

ABSTRACT

A plastic and steel component has been analyzed under repeated loading conditions. Design, experimental and finite element approach has been adopted for the same. Different materials have been explored for improving the life of the component and also the efforts on reducing the stress concentration in the design in increase the life of component. An experimental setup is designed in which component under study is subjected to repeated loading with the help of solenoid actuator and the failure of the component observed with respect to no. of cycles. The acceleration plots and speed of the actuator is correlated with the failure behaviour of component under study. The proposed method is very useful for determining the life of component subjected to repeated loaded and very good correlation is establish between the finite element results and the experimental test data.

KEYWORDS: *Fatigue failure, Finite element method, plastic parts, repeated loading, steel part*

I. INTRODUCTION

The purpose of the present work is to establish the systematic procedure for identifying the failures of the core stop assembly with is operated by solenoid actuator. Here the sequence of failure has been analysed to ensure the life of assembly as per standards and improve the life of the assembly further by taking the corrective actions on the failure modes. Different aspects are analysed such the significant of stress concentration factor on the failure mode and how the life can be improved by changing the design and by reducing the stress concentration. Different materials have been studies for the impact strength and SN curves for selecting the right material for the required life of the components.

H. Nahvi and M. Jabbari [1] have come up with an analytical, as well as experimental approach to the crack detection in cantilever beams by vibration analysis is established. An experimental setup is designed in which a cracked cantilever beam is excited by a hammer and the response is obtained using an accelerometer attached to the beam. Samer Masoud Al-Said [2] has proposed a simple algorithm based on a mathematical model to identify crack location and depth in a stepped cantilever Euler–Bernoulli beam carrying a rigid disk at its tip. The mathematical model that describes the lateral vibration of the beam is derived using the assumed mode method that coalesces with the Lagrange's equation. The proposed identification algorithm utilizes the first three natural frequencies shift of the beam caused by a crack to estimate its location and depth. In addition, the proposed mathematical model is used to illustrate the effect of the crack depth and its location on the dynamic characteristics of the system. Using the commercial finite element (FE) software (ANSYS 8.0), three-dimensional finite element analysis (FEA) is carried out to show the accuracy of the derived mathematical model and to demonstrate the reliability of the proposed crack identification algorithm. The beam centerline is assumed to have only lateral deformation in the Y direction. The analysis showed consistency with the assumed mode results. It showed that the error in concurrent prediction of crack depth and its location using the proposed algorithm is about 10%. B. P. NANDWANA AND S. K. MAITI [3] proposed a method based on measurement of natural frequencies is presented for detection of the location and size of a crack in a stepped cantilever beam. The crack is represented as a rotational spring and the method involves obtaining plots of its stiffness with crack location for any three natural modes through the characteristic equation. The point of intersection of the three curves gives the crack location. Vibration based methods of detection of a crack offer some advantages. They can help to determine the location and size of a crack from the vibration data collected from a single point on the component. When a crack develops in a component, it leads to a reduction in the stiffness and an increase in its damping. Jesús Toribio, Beatriz González and Juan-Carlos Matos [5] analyzed the influence of microstructure on fatigue crack growth was analyzed in steel with slightly hypereutectoid composition. A material constituted of pearlite colonies and a thin layer of proeutectoid cementite (pearlitic steel) was studied in its initial condition (as received). In addition, the same material was analyzed after undergoing a spheroidization treatment obtained by an isothermal treatment on pearlitic steel at 700ºC and heating time of 10h. Results indicate that fatigue crack propagation curve in the Paris region is not modified by the spheroidization process. Fracto metallographic analysis showed a change in the micro mechanism of fatigue, evolving from transcollonial (trying to break pearlite lamellae) in the pearlitic steel to intergranular in the spheroidized steel, where cracking takes place through the layer of proeutectoid cementite. Spheroidization treatment in pearlite produces fragmentation, spheroidal shape and coalescence in the cementite due to the diffusion processes (Chattopadhyay and Sellars, 1982), and these microstructural changes could influence mechanical properties of pearlite. Spheroidization diminishes yield strength, at the same time increasing ductility and fracture resistance. In this way, in pearlitic and spheroidized steel, tensile strength depends on the mean slip distance in the ferritic phase, according to the Hall-Petch equation. Furthermore, fracture toughness in the pearlitic microstructure increases with the decrease of the prior austenite grain, whereas spheroidized steel does so with the increase of the mean free path between cementite carbides.

This paper is organized as below:

I. Introduction to cover the background of research
II. Methodology of understanding the pain area, analyzing the components, design calculations and correlation of the results
III. Results and Discussion covers the experimentation part of the research works and the correlations between experimentation and FEA results.

II. METHODOLOGY

Solenoid stopper assembly is designed for the required life of all the components of assembly and for which each component is design and analyzed. Fig 1 shows the major components of core stop assembly which are subjected to repeated loading condition due to the movement of solenoid plunger. Solenoid force is determined based on the requirement of final product and according design calculations are done. When the solenoid is energized plunger is pulled in and at top dead centre position current is topped to the solenoid coil. Along with the plunger spring is also getting compressed when the solenoid is pulled in and store the energy so at top dead centre position when the solenoid current is stopped, spring will release its energy and will come back to its original position. This movement of plunger happens at very high speed and the total travel time for the plunger from top dead centre to original position is less than 60ms. This results in very high impact force on the structural components of the core stop assembly. High stresses are induced in all the components because of the impact force.

There are three different components which are likely to fail under repeated loading shown in Fig.1 Stopper is made up plastic and has to be analysed under the impact load for required number of cycles. Frame is mounted firmly to the structure and undergoes vibration because of repeated loading condition. Link is subjected to tensile stresses in the first half cycle when the plunger is pulled in and then it is subjected to compressive stresses in the next half cycle when spring releases its energy.

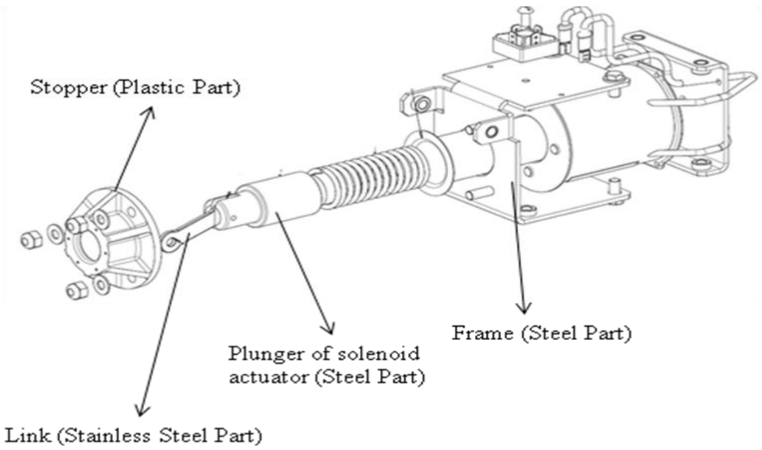

Fig 1. Main Components of Stopper Assembly

It is important to determine to impact force on the stopper when the solenoid actuator is operated and that impact force is taken as an input for optimizing the stopper assembly components. Fig 2 shows the cross-sectional view of the stopper assembly with two positions of plunger. Fig 2(a) show the initial position and Fig 2(b) top dead centre position.

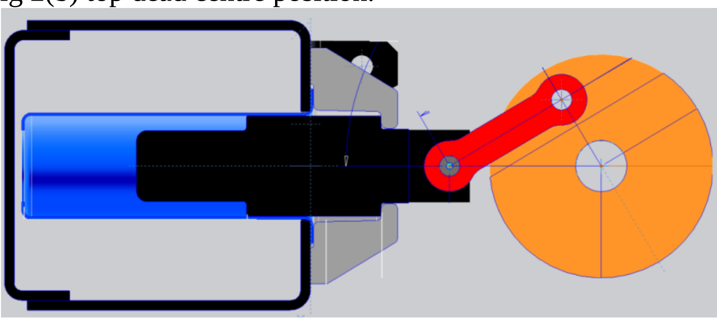

Fig 2(a) stopper assembly at initial position

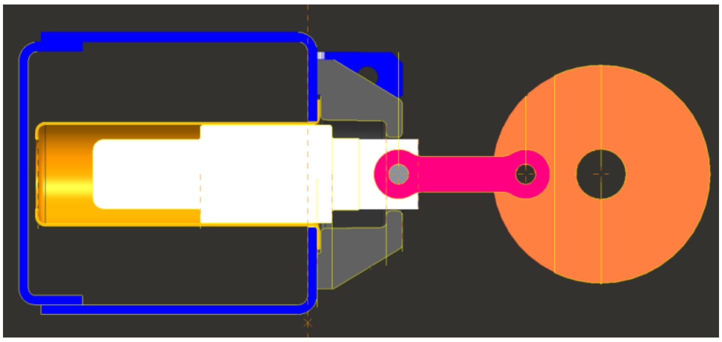

Fig 2(b) stopper assembly at top dead centre (TDC) position

Table 1 shows the calculations for impact force. This data is used for finite element analysis using Ansys workbench and stress have been compared for different design of stoppers.

- $F=kx$
- ½ Mv2 = ½ kx2 (for Plunger)
- ½ Iω2 = ½ kx2 or
- F = (kM)1/2v + (kI)1/2 ω
    - M & I were derived from the part drawings
    - v = 48 in/sec, ω = 41.6 rad /sec (from CAD layout and v)
    - k = 160,000 lb/in (derived from static FEA model)

Table 1 : Calculation for impact force due to the movement of plunger in the solenoid assembly

Input			
Parameters	Symbols	Values	Units – IPS
Mass Of 'Weight'	m1	5.0	Lbs
Mass Of 'Shaft'	m2	2.0	Lbs
Inertia Of Shaft	I1	0.3	lbf-Inch^2
Inertia Of Wt	I2	5.0	lbf-Inch^2
Angular Velocity	Ω	2350.0	degree/Sec
Angular Velocity	Ω	41.1	rad/Sec
Calculations			
Max Principal Stress	Σ	22570.0	Psi
Load	F	3350.0	Lbf
Deformation	X	0.0202	Inch
Material Stiffness	K = F/X	166006	lbf/Inch
Kinetic Energy	E1=1/2(K*X^2)	33.8	lbf-Inch
Total Moment Of Inertia	I=I1+I2	5.3	lbm-Inch^2
Angular Velocity	Ω	6.5	Rpm
Kinetic Energy	E2=1/2(I*ω^2)	4473.3	lbf-Inch^2-Rev^2 /Sec^2
Total Rotating Mass	M=m1+m2	7.0	Lb
Linear Velocity	V	12.7	Inch / Sec
Kinetic Energy	E3=1/2(M*V^2)	563.0	lb-Inch^2/Sec^2
Linear Acceleration	A	211.4	Inch / Sec^2
Radius of Rotation	R	1.9	Inch
	√(kM)	1078.0	
	√(kI)	938.0	
Output			
Parameters	Symbols	Values	Units
Impact Force	F = M * a	1479.7	Lbf
FEA KE	E1=1/2(K*X^2)	33.8	lbf-Inch
Angular Kinetic Energy	E2=1/2(I*ω^2)	4473.3	lbf-Inch^2-Rev^2 /Sec^2
Linear Kinetic Energy	E3=1/2(M*V^2)	563.0	lb-Inch^2/Sec^2
Angular Velocity	ω =X*√(K/I)	3.57	
Deformation	X=ω*√(I/K)	0.04	
Impact Force	F= ((V*√(kM) + (ω*√(kI))	3387.00	

2.1. Design of Link

It is the critical components of the complete switching assembly. Link is subjected to tensile stresses in the first half cycle when the plunger is pulled in and then it is subjected to compressive stresses in the next half cycle when spring releases its energy as shown in Fig 3.
Different geometries and material have been explored for designing the link in order to make sure that it passes required no. of operations.

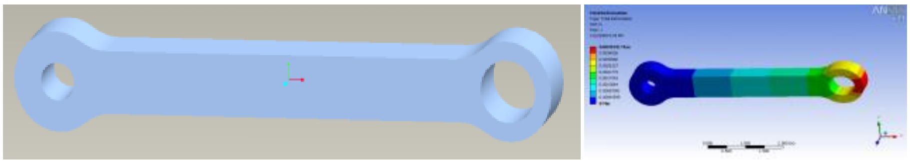

Fig. 3(a) link 1 design and simulation results

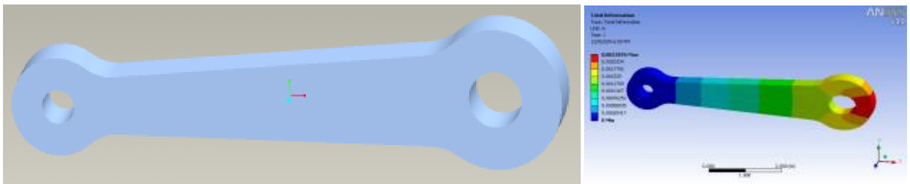

Fig. 3(b) link 2 design and simulation results

Analysis summary

Table 2 Analysis summary of link1 and link2

Parameter	Bearing Load Applied	Stress	Deformation	Fatigue Life
Unit	Lbf	Psi	Inch	No of cycles
Link 1	1236.5	26832	0.004	≈1000
Link 2	1236.5	8891	0.002	≈12000

Link2 design is better and has 20% more life compared to Link1
4 different material are studied and understood the effect of those material on the life of the components considering link1 geometry

Table 3 Material properties for aluminium and stainless steel grades

Material	**Density**	**Ultimate Tensile Strength**	**Tensile Yield Strength**	**Modulus of Elasticity**	**Poisson's Ratio**
Unit	**lb/in³**	**psi**	**psi**	**psi**	
Aluminium 6061 T6	0.0975	44950	40020	9.99E+06	0.33
Aluminium 7075 T6	0.102	83000	73000	1.04E+08	0.33
Stainless Steel-17-4PH-1075	0.283	155000	135000	2.85E+07	0.272
Stainless Steel-17-4PH-1150	0.284	145000	125000	2.85E+07	0.272

Max principle stresses are also found using FEA for all the 4 materials and SN curve are compared for both the grades of aluminium for determining the life of the component based on maximum principle stress.

Table 4 Max principle stress and deformation results for aluminium and stainless steel grades

Material	**Density**	**Ultimate Tensile Strength**	**Tensile Yield Strength**	**Modulus of Elasticity**	**MPS @ Load 1517.6 lbf**	**MPS @ % of Yield**	**Deformation @ 1517.6 lbf**
	lb/in³	**psi**	**Psi**	**psi**	**psi**	**%**	**Inch**
Aluminium 6061 T6	0.0975	44950	40020	9990500	33191	83	0.00451
Aluminium 7075 T6	0.102	83000	73000	104000000	33191	45	0.00433
Stainless Steel-17-4PH-1075	0.283	155000	135000	28500000	32872	24	0.00157
Stainless Steel-17-4PH-1150	0.284	145000	125000	28500000	32872	26	0.00157

From the above table it is evident that between two grades of Aluminium 7075 T6 is better than Aluminium 6061 T6 as the stresses for 40% lower and also life is 10 times more when compared on the SN curve.

International Journal of Scientific Research and Management Studies (IJSRMS)
ISSN: 2349-3771 **Volume 2 Issue 4, pg: 164-174**

2.2. Design and Simulation of Frame

Different designs have been evaluated and FEA has been carried out to study the stress on the component and best design has been picked. Fig 4 shows three different designs.

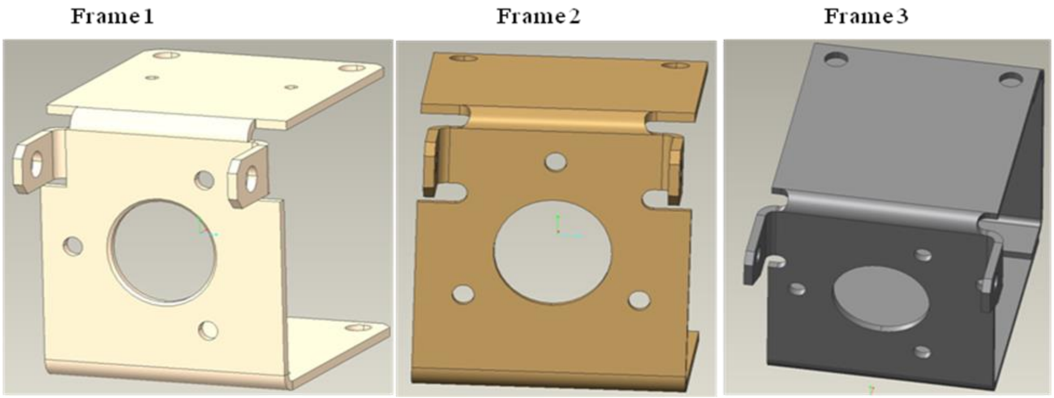

Fig 4 frame designs

Frame 1 has sharp corner on the bends which are converted into round in frame 2 and 3. Those are analyzed using Ansys and max stresses are determined from that. Fig 5 shows the FEA model of frame for all the three designs.

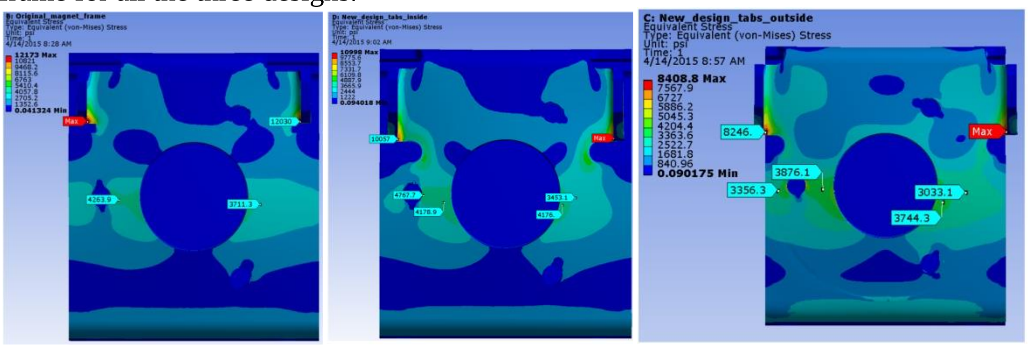

Fig 5 FEA models of Frame1, Frame 2 and Frame 3 respectively

From the FEA analysis it has been observed that stresses in Frame 2 are 9.6% lower compared to Frame 1 and stresses in Frame 3 are 31% lower than Frame 1. It can be concluded from the analysis that stress concentration has significant effect on the life of the component and as the corners are rounded and relief is decreased stresses reduces significantly.

2.3. Design of Stopper

FEA has carried out with below boundary conditions:

- 1000 pounds applied at the plunger interface.
- Pinned boundary conditions at the bolt head locations.
- Core Stop material = ZYTEL 70G33HSL (Yield strength = 18,000 psi)
- The mesh was refined in the areas of high stress.

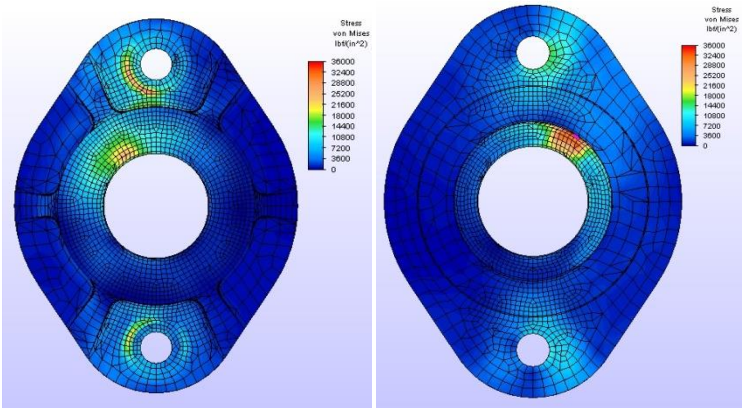

Fig 6 FEA models of stopper design 1

The stress distribution from 1000 pounds concentrated near a rib is shown at the right. The maximum estimated stress was 26,000 psi tension (top side near the bolt hole) & 36,000 psi compression (bottom near the load).

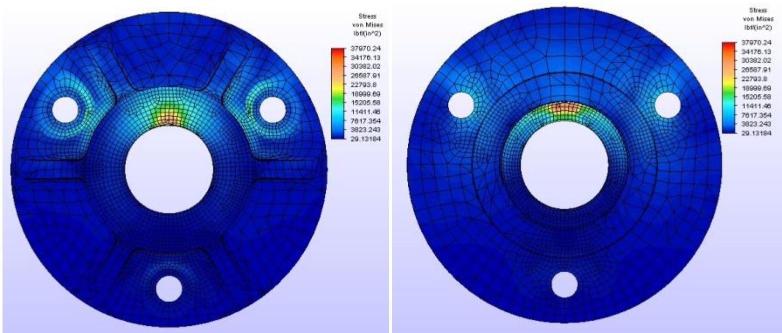

Fig 7 FEA models of stopper design 1

The stress distribution from 1000 pounds concentrated opposite a bolt hole is shown at the right. The maximum estimated stress was 18,000 psi tension (top side near load point) & 34,000 psi compression (bottom near load point).

Table 5 Comparison of Design#1 and Design2 stopper results if the impact load found from the kinematic simulation (3,300 lbs) were statically applied

Peak Tensile Stress (psi) From 1,000 Pounds.

	Uniform Load	Load Near Hole	Load Near Rib	Load Opp Hole
Design #1	59,400 *	79,200 *	85,800 *	N/A
Design #2	42,900 *	85,800 **	85,800 **	59,400 **

* = High Stress Near Bolt Hole ** = High Stress Near Load Point

Design and simulation summary for Design#1 and Design#2 stopper

- Comparing the (more realistic) uniform load case of Designs #1 & #2:
- The estimated stress in Design #2 is 28% lower than that of Design #1.

Different material are explored to increase the life of components as shown in Table 6

Table 6 material comparison for different grades of zytel

Material	Modulus (psi)	Yield Strength (psi)	Impact Strength ft-lb/in
70G33	900,000	18,000	2.5
ST801	125,000	6,000	20

The loading condition is impact load situation, hence super toughened nylon i.e. Zytel ST801 has impact strength that of 8 times of Zytel 70G33.

III. Results And Discussion

3.1. Position Vs Time set up for solenoid actuator and stopper assembly

Total travel of the solenoid actuator is between 60-120ms. Position vs time plot help to determine the velocity and acceleration of the plunger of the solenoid actuator which helps in calculating the speed and hence the impact force on the stopper.
Set up has been made with the help of transducer and suitable hardware and software so when the pulse is given to solenoid it captures the data with the resolution of 1ms with respect to stroke of the plunger.

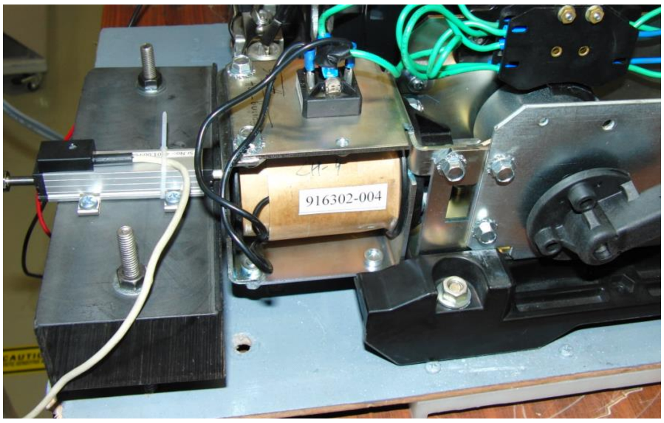

Fig 8 Position vs time set up

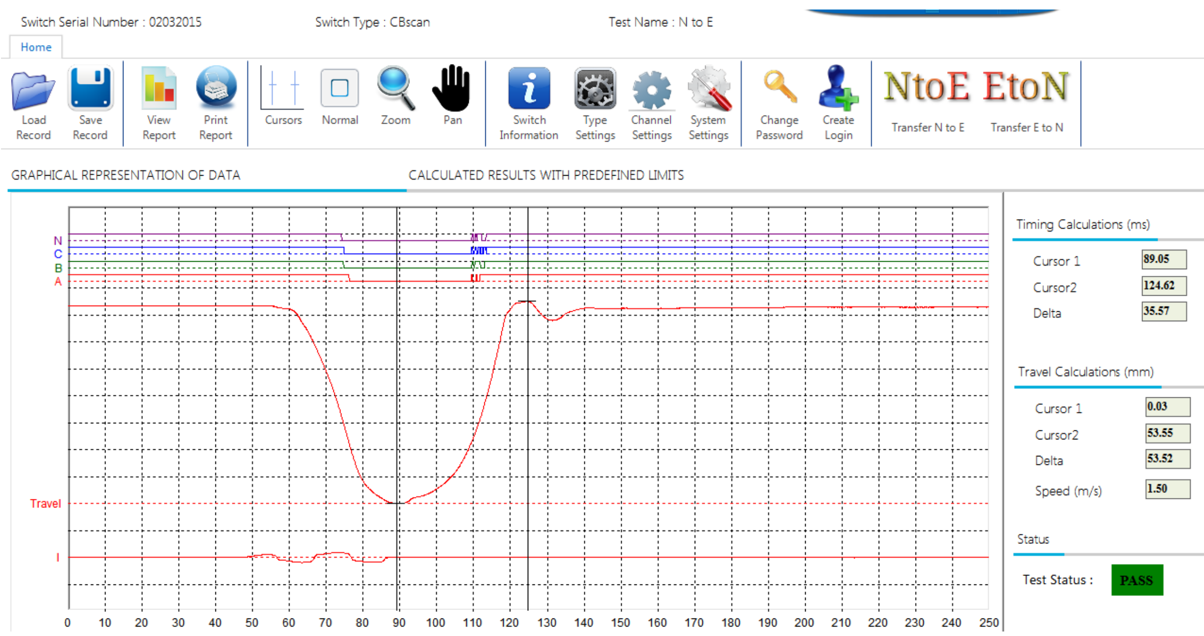

Fig 9:- Position vs time plot for the stopper assembly

Above graph gives the speed and hence the impact force can be calculated.

3.2. Life Test

The life cycle test is performed on the stopper assembly by giving plus to the solenoid actuator and in one plus solenoid will complete its one operation. Voltage is set on the transformer as per the rating of the solenoid coil and input pulse is given to operate the coil. Endurance test has been carried out to

determine the life of all the components of stopper assembly. Frequency of the operation has been set to 1 operation per minute to comply with the applicable standard.
When the life test is carried out on the equipment under test with the link 1 and frame design 1 and below is the observations.
After 9000 operations link there was improper functioning of the actuator and when the test is stopped it has been observed that the hardware for the stopper has loosen up due to vibration and repeated loading. When investigated it has been found that the normal hex nuts needs to be replaced with the Nylon nuts. Testing has been continued after replacing the nuts and tightened with the proper torque. Fig 10 shows the image of stopper hardware loosening

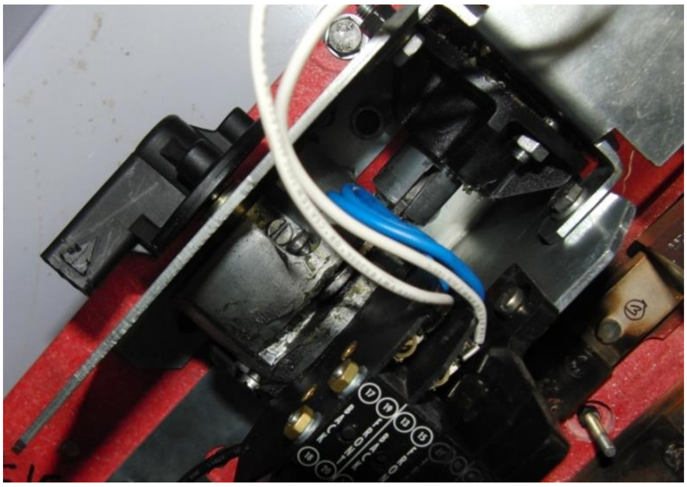

Fig 10:- Stopper hardware loosen after 9000 operations

After 14000 operations crack has been observed in the Frame (design1) and there was a failure on one side of frame. It has been evident that the failure occurred because of the stress concentration and high stresses. Fig 11 shows the failure of frame (design 1) due to the stress concentration

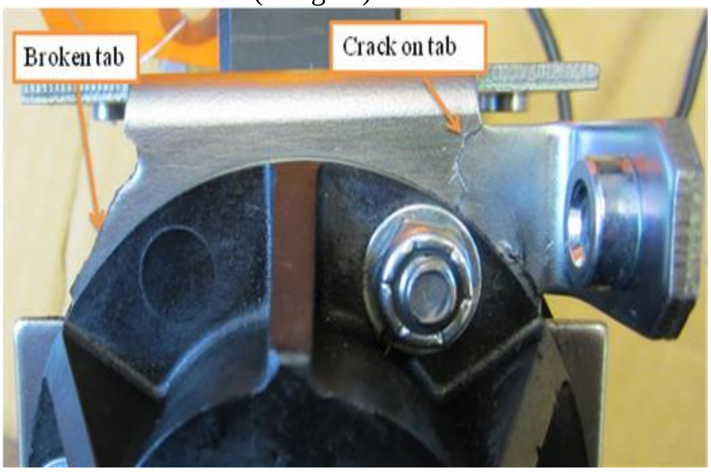

Fig 11:- Frame 1 break after 14000 operations

Another prototype is built with the Frame 3 design which shows 31% improvement in the stresses and started life test. There was no failure in the frame until 25000 operations and test has been stopped as it passes the required life with FOS of 25%.

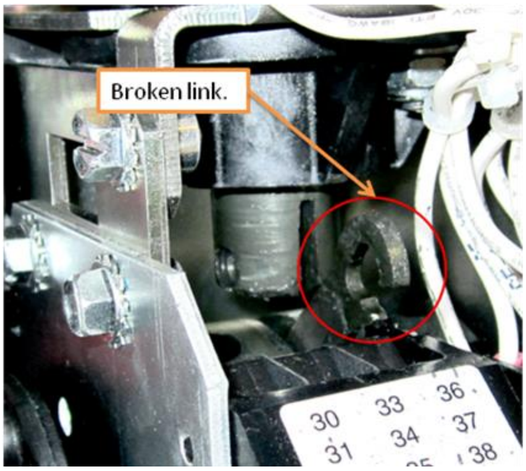

Fig 12:- Aluminium 6061 link broke after 16000 operations

After 16000 operations there was a failure in the link1 as shown in Fig 12. The link was made of Aluminium 6061 T6. When in another prototype the link was replaced with Aluminium 7075 T6 material it was successfully completed 28000 operations before it failed so it can be concluded that Aluminium 7075 T6 meets the requirement and pass 20000 operations.

For experimentation purpose stainless steel link is also tested on the stopper assembly and it could cross 40000 operations without fail and test has been stopped.

IV. CONCLUSIONS

A systematic approach of failure mode of different components has been studied. Good correlation in the theoretical calculations and simulation results is achieved for determining the impact load. All the parts of core stop assembly were analysed to ensure minimum life of 20,000 operations. Experimental set up help in verifying the assembly life and identifying the life of each component. Material plays vital role in determining the life of component and alternate materials are identified to enhance the life along with the design changes. Effect of stress concentration on the fatigue life of the component is studied and rectified by changing the localized area to reduce stress concentration. There has been very good correlation in the calculations, FEA results and test results for determining the impact force and hence the stresses on the component and hence proved that all the components are safe for the life of 20,000 operations for the assembly.

ACKNOWLEDGEMENTS

I wish to express my sincere thank to Prof Khan for guidance and encouragement in carrying out project work. My sincere thanks to Mr. Subrahmanyam Jana, Group Program Manager from Emerson Innovation Centre – Pune and Mr. Richard Encelewski, Manager Switch Design for kind cooperation during the execution of project.

REFERENCES

[1]. H. Nahvi, M. Jabbari, (2005) "Crack detection in beams using experimental modal data and finite element model", International Journal of Mechanical Sciences 47 pp 1477–1497
[2]. Samer Masoud Al-Said, (2007) "Crack identification in a stepped beam carrying a rigid disk", Journal of Sound and Vibration 300 pp 863–876
[3]. B. P. Nandwana and S. K. Maiti, (1997) "Detection of the location and size of a crack in stepped cantilever beams based on measurements of natural frequencies", Journal of Sound and Vibration 203(3), 435-446
[4]. Q.S.Li, (2001) "Vibratory characteristics of multi step beam with an arbitrary number of cracks and concentrated masses", Applied Acoustics 62 pp 691-706
[5]. Jesús Toribio, Beatriz González and Juan-Carlos Matos, Influence of the microstructure of eutectoid steel on the cycle crack propogation, International Journal of Fracture DOI 10.1007/s10704-011-9633-7.
[6]. Farhad B. Bahaideen, "Fatigue Behaviour of Aluminum Alloy at Elevated Temperature", Modern applied science, Vol 3 No 4

[7]. R.O. RITCHIE,(1999) Mechanisms of fatigue-crack propagation in ductile and brittle solids, International Journal of Fracture 100: 55–83.
[8]. C. M. Sharanaprabhu, Shashidhar K. Kudari,(2010) "Mixed-mode crack initiation direction for elastic-plastic materials", International Journal of Engineering, Science and Technology Vol. 2, No. 11.
[9]. Norman E. Dowling,(2004) "Mean Stress Effects in Stress-Life and Strain-Life Fatigue", Society of Automotive Engineers, Inc
[10]. Michael D. Sangid (2013) "The physics of fatigue crack initiation" International Journal of Fatigue, Volume 57, PP 58-72
[11]. Kianoosh Poorkazem, Dianyi Liu and Timothy L. Kelly* (2015) "Fatigue resistance of a flexible, efficient, and metal oxide-free perovskite solar cell" Journal of Materials Chemistry A, Issue 17

AUTHORS SHORT BIOGRAPHY

Sachin Shah was born in Jalgaon, India, in 1979. He received the Bachelor in mechanical engineering degree from the University of Pune, Kopargaon; in 2001 He is currently pursuing the Masters degree with the Department of Mechanical Engineering, Pune. His research interests include study of fatigue failure in plastic and steel components.